

## Delocalizing transition of multidimensional solitons in Bose-Einstein condensates

Bakhtiyor B. Baizakov<sup>y</sup> and Mario Salerno

Dipartimento di Fisica "E.R. Caianiello" and Istituto Nazionale di Fisica della Materia (INFM),  
 Università di Salerno, I-84081 Baronissi (SA), Italy  
 (March 22, 2002)

Critical behavior of solitonic waveforms of Bose-Einstein condensates in optical lattices (OL) has been studied in the framework of continuous mean-field equation. In 2D and 3D OLs bright matter-wave solitons undergo abrupt delocalization as the strength of the OL is decreased below some critical value. Similar delocalizing transition happens when the coefficient of nonlinearity crosses the critical value. Contrarily, bright solitons in 1D OLs retain their integrity over the whole range of parameter variations. The interpretation of the phenomenon in terms of quantum bound states in the effective potential is proposed.

PACS numbers: 03.75.Fi, 05.30.Jp, 05.45.-a

## I. INTRODUCTION

Bose-Einstein condensates (BEC) display remarkably rich nonlinear wave phenomena, among which solitons are particularly interesting. To date both common types of solitons, bright and dark, are experimentally realized in BECs, respectively, with attractive and repulsive interaction forces [1,2]. Theoretical studies of the properties of matter-wave solitons has resulted in successful description of basic features of soliton dynamics in BEC [3].

Considerable effort is being devoted to investigation of BEC in periodic potentials created by laser standing waves – so called optical lattices (OL). Subjecting a BEC to a periodic potential leads to a number of interesting phenomena, including the formation of a specific class of localized modes called gap solitons. The definition ‘gap’ refers to the fact that this type of solitons exist in the band gaps of the matter-wave spectrum. Conceptually important point here is that, the gap solitons can be composed of repulsive atoms, which makes them favorable against bright solitons in continuous attractive BEC tending to collapse at high atomic densities.

After the first discussion of the possibility of bright solitons in repulsive BEC loaded in OL [4], substantial theoretical research was performed aimed at understanding their development and properties [5]. One of the recent advances in this direction has been the proof of the possibility of matter-wave solitons in two- and three-dimensional (2D and 3D) OLs. Particularly, the emergence of multi-dimensional gap solitons in repulsive BEC arrays due to the phenomenon of modulational instability was demonstrated in [6]. Different modes of stable 2D gap solitons in OLs were shown to exist by numerical solution of the corresponding 2D Gross-Pitaevskii equation [7]. Multidimensional solitons in media governed by the self-focusing cubic nonlinear Schrödinger equation (NLSE) with a periodic potential, of which an attractive BEC in OL is a particular example, are studied in [8] by means of the variational approximation and direct numerical simulations.

While have not been experimentally realized yet, bright matter-wave solitons in OLs currently are among

the intensively explored subjects in BEC. An important aspect of OLs is that they provide a unique possibility to investigate the behavior of localized excitations and solitons in both continuous and discrete ends of the spectrum by adjusting the strength of the OL. A fundamental issue that the cubic NLSE does not support stable solitons in dimensions higher than one, while its discrete analog does, can be addressed more effectively involving the BEC in OL. One relevant problem – the delocalizing transition of BECs in deep 2D OLs has recently been investigated in the framework of discrete NLSE [9]. The analysis of Ref. [9] is relevant to the tight-binding approximation, when the BECs in neighboring lattice sites are weakly linked. This approach also relies on the possibility, that the tunneling amplitude between OL sites can be accurately determined. In the case of uniformly loaded OL the tunneling amplitude can be estimated using the Wannier function basis [10]. However, in the case of localized excitations involving just few lattice sites with significantly different occupation numbers, calculation of the tunneling amplitude becomes difficult.

The aim of this paper is twofold. From one side we present a detailed numerical investigation of the delocalizing transition beyond the tight-binding approximation, when the system is described by the continuous mean-field equations. To this regard we provide both analytical and numerical evidences for the existence of stable multidimensional solitons in OLs, and we study the fade and recovery of the solitonic structures as the strength of the optical lattice or coefficient of nonlinearity adiabatically varies in time. The major topic of interest will be a critical behavior of solitonic waveforms in a periodic potential, expressed as sudden disintegration of the soliton when the system parameters attain particular values. This will be done for BECs with both positive and negative scattering lengths. From this study it emerges that the variational ansatz while correctly predicting the stabilization of solitons due to the OL, it fails to predict the existence of a delocalizing transition.

From the other side, we address to the physical mechanism underlying the delocalizing transition. To this regard we propose a quantum interpretation of the phe-

nonmonotonic, by showing that the delocalizing transition is associated to the disappearance of bound states from the soliton effective potential in the underlying periodic Schrödinger equation. Since in one dimension any potential well can support at least one bound state (this is true even for infinitesimal well depths), the above interpretation automatically implies that 1D solitons cannot undergo delocalizing transitions. This is indeed what we find for the 1D case. In particular we show that by decreasing the strength of the OL or the nonlinearity in the system, the soliton becomes very extended (in the limit of zero nonlinearity it reduces to a Bloch state at the edge of the Brillouin zone), but always recovers its original shape when the parameters are reversed. In contrast, in 2D and in 3D cases, we find that there is always a critical value of system parameters below which the recovering of the soliton becomes impossible i.e. the soliton irreversibly disintegrates into extended states. By approximating the soliton effective potential with a suitable solvable potential and by adopting a variational ansatz description for the soliton, we show that the above bound state interpretation leads to an analytical expression for the occurrence of the delocalizing transition which is in good agreement with direct numerical simulations of the Gross-Pitaevskii equation, this providing support for our approach.

We remark that the proposed mechanism for the delocalizing transition is general and expected to be valid also for multidimensional intrinsic localized modes or discrete breathes of nonlinear lattices, as well as for multidimensional soliton solutions of the NLSE with nonlocal interactions.

Finally, we have explored the role of dimensionality by comparison of results for 2D and 3D OLs. The advantage of the present approach is that, all the system variables are readily connected to actual physical parameters (e.g. the OL strength to the laser intensity and the coefficient of nonlinearity to the atomic scattering length, etc.), which makes the experimental verification more feasible.

The paper is organized as follows. In Sec. II we introduce the model and derive variational equations for soliton parameters. Then we check the validity of VA equations by comparing with direct numerical solution of the Gross-Pitaevskii equation. In Sec. III we propose a physical mechanism associating the existence of solitons and their delocalizing transition with quantum bound states in the effective potential. The existence region for 2D solitons is presented. In Sec. IV we discuss the possibility of experimental observation of the delocalizing transition of solitons. Finally, in Sec. V we conclude the results of this study.

## II. THE EXISTENCE OF SOLITONS IN PERIODIC POTENTIALS

The existence, stability and some other properties of solitons in 1D periodic potentials are explored in the

context of repulsive BEC in OLs [4,5]. Solitons in self-focusing NLSE with a 1D periodic potential, with relevance to particular problems of nonlinear optics is considered in [11]. While the subject is well understood in 1D case, multidimensional solitons in periodic potentials are in early stage of research [6-8]. Below we analyze the existence of multidimensional solitons in periodic potentials in the framework of the variational approximation (VA) for both attractive and repulsive interactions. The results will then be compared with numerical simulations of the full problem. We remark that the VA analysis based on a Gaussian waveform was recently considered in Ref. [8] for the case of 2D BEC with attractive interactions. In this case it was shown that bright solitons are well approximated by Gaussian profiles, this being particularly true when all the matter is confined into a single cell of the OL (single cell solitons). In the case of BEC with repulsive interactions, however, satellite peaks appear in the soliton waveform and the VA based on a Gaussian ansatz leads to wrong results. In this case we will show that a Fraunhofer diffraction pattern is a better ansatz for the soliton shape, leading to VA equations which are in good agreement with numerical simulations.

### A. Basic equation

The analysis will be based on the mean-field Gross-Pitaevskii equation (GPE) for the macroscopic wave function of the condensate  $\psi(\mathbf{r};t)$ , which describes the properties of a dilute gas near-zero temperature BEC [12]

$$i\hbar \frac{\partial \psi}{\partial t} = -\frac{\hbar^2}{2m} \nabla^2 \psi + V_{\text{ext}}(\mathbf{r};t) + g|\psi|^2 \psi; \quad (1)$$

where  $m$  is the atomic mass,  $g$  is the nonlinear coupling parameter related to the  $s$ -wave scattering length  $a_s$  through  $g = 4\pi\hbar^2 a_s/m$ ,  $V_{\text{ext}}(\mathbf{r};t)$  is the external potential, generally consisting of harmonic confinement plus periodic potential of the OL

$$V_{\text{ext}}(\mathbf{r};t) = \frac{m}{2} \dot{\mathbf{r}}_i^2 + U \cos(2k_L \mathbf{r}_i); \quad (2)$$

where  $\mathbf{r}_i = x; y; z$  and sum over  $i$  is assumed. We shall be interested in the behavior of localized excitations, occupying few central unit cells of the OL, when the effect of confining parabolic potential is not essential. Therefore, in what follows we assume the presence of the OL only. For convenience we rescale the Eq.(1) by introducing the dimensionless variables  $\mathbf{r}_i \rightarrow k_L \mathbf{r}_i$ ,  $t \rightarrow (\hbar k_L^2 / (2m)) t \equiv \tau$ ,  $U \rightarrow U/E_r$ ,  $\dot{\mathbf{r}}_i^2 \rightarrow \dot{\mathbf{r}}_i^2 / n_0$ . Where  $k_L = 2\pi/\lambda$ ,  $E_r = (\hbar^2 k_L^2 / (2m))$ ,  $\lambda$ ;  $k_L$  being the laser wavelength and wave vector correspondingly,  $n_0$  is the density of BEC. We also designate the coefficient of nonlinearity as  $g = 8\pi\hbar^2 a_s k_L^2$ . Then we have Eq.(1) in the form

$$i \frac{\partial \psi}{\partial \tau} = -\frac{1}{2} \nabla^2 \psi + V_{\text{ol}}(\mathbf{r};\tau) + |\psi|^2 \psi; \quad (3)$$

where  $V_{ol}(r;t) = V[\cos(2x) + \cos(2y) + \cos(2z)]$  is the OL potential.

### B. Variational approach

To deal with compact expressions, we explicitly consider the 2D case, since the extension to 3D is straightforward. We look for the stationary solution of Eq.(3) in the form

$$\psi(x,y;t) = U(x,y) \exp(-i\mu t); \quad (4)$$

where  $\mu$  is the chemical potential. Then the following equation determines the time-independent solution  $U(x,y)$

$$-\nabla^2 U + U + V_{ol}(x,y)U + U^3 = 0; \quad (5)$$

Following the standard procedure of the VA [13,14], we consider the effective Lagrangian

$$L = \frac{1}{2} \int_{-\infty}^{\infty} \int_{-\infty}^{\infty} (|\nabla U|^2 - U^2 - V_{ol}(x,y)U^2 - \frac{1}{4} U^4) dx dy \quad (6)$$

which generates the Eq.(5) by minimization  $\delta L = 0$ . The next step of the variational approach involves the choice of a suitable trial function – ansatz for the solution. As we shall see later, solitonic waveforms in attractive and repulsive BECs in the periodic potential have different spatial features. This implies the choice of different trial functions, which we shall consider separately.

#### 1. Attractive BEC

The nature of interatomic forces in BEC can be attractive or repulsive, which leads to very different properties of corresponding BECs [12]. The attractive case corresponds to the negative sign of the s-wave scattering length  $a_s$ , and the underlying GPE has a self-focusing nonlinearity ( $\gamma < 0$ ). The collapse of BEC at some critical number of atoms  $N_{col} \approx 1400$  is the main consequence of the self-focusing nonlinearity [12]. The presence of a periodic potential, however, significantly changes the situation and leads to stable localized states. In moderately strong and weak periodic potentials (which is the case at delocalizing transition point considered below) multidimensional solitons have a single cell structure and are well described by the VA with Gaussian ansatz [8]

$$U(x,y) = A \exp\left[-\frac{a}{2}(x^2 + y^2)\right]; \quad (7)$$

where the amplitude  $A$  and width parameter  $a$  are fixed by the total number of atoms in the condensate  $N = \int_{-\infty}^{\infty} \int_{-\infty}^{\infty} |U(x,y)|^2 dx dy = A^2/a$ . Variational equations are derived by substituting the ansatz (7) into the effective

Lagrangian (6), performing the spatial integration and subsequent minimization with respect to variables  $A$  and  $a$ . The equations associate the parameters of the soliton with the total number of atoms, strength of the OL, and chemical potential of the BEC

$$N = \frac{4}{a} \left(1 - \frac{2}{a^2} e^{-1/a}\right); \quad \mu = \frac{2}{a} \left(2 - a\right) e^{-1/a} - a; \quad (8)$$

A noteworthy property of Eq.(8) is that, for a given strength of the OL  $V$  there exists a minimal norm  $N_{min} = \frac{4}{a^2} (1 - 8e^{-2})$  attained at  $a = 1/2$ , below which the localized solutions do not exist, as illustrated in Fig.1. The threshold vanishes for stronger OLs,  $V > V_{cr} = e^2/8 = 0.92$ . The existence of solitons in 2D attractive BEC from above is limited by the onset of collapse at the critical norm  $N_{col} = 4$  predicted by VA [15] (the exact value being  $N_{col} = 11.6993$  [16]).

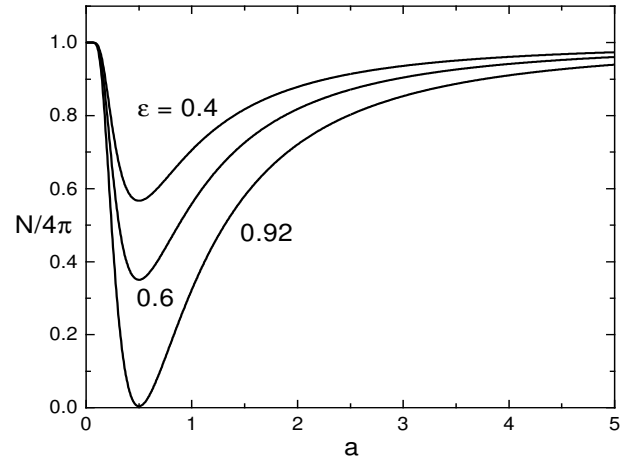


FIG. 1. The Eqs.(8) predict two localized solutions for a given norm  $N$ , one of which ( $a > 1/2$ ) is stable and the other ( $a < 1/2$ ) is unstable.

The VA predicts two localized states with different widths for a given norm  $N_{min} < N < N_{col}$ . The stability of these two solutions can be inferred from the Vakhitov-Kolokolov criterion [17]. According to this criterion, the branch of solutions with  $a > 1/2$  has the negative slope  $dN/da < 0$ , and therefore is stable. The other branch ( $a < 1/2$ ) appears to be unstable.

#### 2. Repulsive BEC

The main feature of a soliton of repulsive BEC ( $\gamma > 0$ ) in a periodic potential is that, it is composed of a central peak and symmetrically spaced satellites residing in neighboring cells of the OL. The issue of vital importance for VA is the adoption of a suitable ansatz. A Gaussian waveform obviously is not satisfactory in this case since it doesn't take into account the composite shape of solitons. We introduce the following ansatz

$$U(x;y) = A \frac{\sin(ax)}{ax} \frac{\sin(ay)}{ay}; \quad (9)$$

which accounts for the satellites, and has the advantage of yielding simple VA equations. An analytical transformation similar to the previous case leads to following set of equations

$$N = \frac{3^2}{2a^3} \frac{3''}{1}; \quad = \frac{2''}{a} (2 - a) - \frac{2}{3}a^2; \quad (10)$$

The relation connecting the norm and soliton parameters in this case is  $N = \frac{1}{2}A^2/a^2$ , which yields in combination with Eqs.(10)

$$A = \frac{h}{2} \frac{9N^{3/2}''}{(N + 3^2)} \frac{i_{1=3}}{1}; \quad (11)$$

Unlike the attractive case, the ansatz Eq.(9) yields a single set of soliton parameters  $a; A$  for a given norm  $N$  and strength of the O.L. In the next subsection we compare the prediction of the VA with direct numerical solution of the GPE (3).

### C. Comparison of VA and PDE simulations

Validity of the VA is usually verified by comparison with the results of direct numerical solution of the underlying PDE. Below we solve the Eq.(3) by split-step procedure using the multidimensional fast Fourier transform [18] on the grids of 512, 256x256 and 128x128x128, respectively in 1D, 2D and 3D cases. The domain size and time step are  $x; y; z \in [-4; 4]$ ,  $t = 0.001$ . The essential point is the use of absorption on the domain boundaries to prevent re-entering of linear waves emitted by the soliton during its formation (or under perturbations) into the integration area.

The comparison between VA and PDE simulations can be done in different ways. We consider the situations more relevant to experiments, namely, we change the strength of the O.L. or the coefficient of nonlinearity (which is equivalent to changing the norm  $N$  at constant  $\mu$ ), and follow the evolution of the soliton's amplitude according to PDE (3). Then we correlate the numerically obtained dependence  $A(\mu)$  or  $A(N)$  with analytical prediction of VA Eqs.(8,10). Below we perform the comparisons for 2D case.

#### 1. Attractive case

At first we need to generate a stable 2D soliton of Eq.(3). For this we insert the Gaussian waveform (7) with parameters specified by VA (see Fig.1) into the Eq.(3) as the initial condition. The waveform undergoes some evolution and attains the stable state as shown in Fig.2.

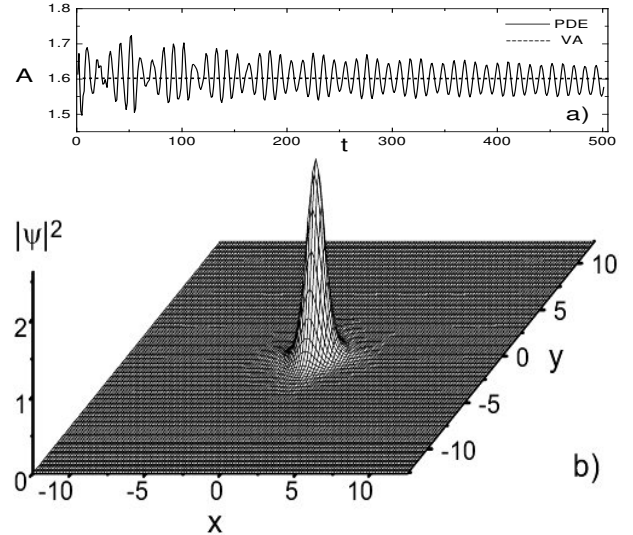


FIG. 2. The Gaussian waveform Eq.(7) with parameters prescribed by VA  $A = 1.6$ ;  $a = 1.3$ ;  $N = 2$ , inserted as initial condition to Eq.(3) evolves into a stable 2D soliton, performing transient oscillations. The strength of O.L. is  $\mu = 0.92$ . a) Comparison VA vs. PDE, b) stable 2D soliton of attractive BEC.

The stability of multidimensional solitons, being a very important issue, is worth of special investigation. Here we refer to our numerical tests, which show that a small deformation of the soliton causes weak oscillations around the stable state. After sufficiently long time the waveform relaxes back to its original shape proving that the stable state is a fixed point, i.e. the soliton is linearly stable. The tests also involve the long-time propagation of a fundamental soliton with PDE for a period much exceeding the characteristic time of the problem.

After the stable 2D soliton is created, we use it as initial condition for Eq.(3) and follow the further evolution under time-dependent parameters  $\mu(t)$  or  $\mu(t)$ . An important point to be stressed here is the condition of adiabaticity in variation of parameters. In the present context, the adiabaticity refers to the situation, when the variation of parameters does not excite collective modes of the condensate, which means that the ramp times should satisfy the condition  $t_{\text{ramp}} \gg \hbar/\mu$ . In our dimensionless units the above condition implies  $t_{\text{ramp}} > 50$  for a typical condensate with chemical potential of  $\mu = 200$  Hz. The soliton's amplitude as a function of the coefficient of nonlinearity, obtained from PDE simulations and compared with the prediction of VA is presented in Fig.3.

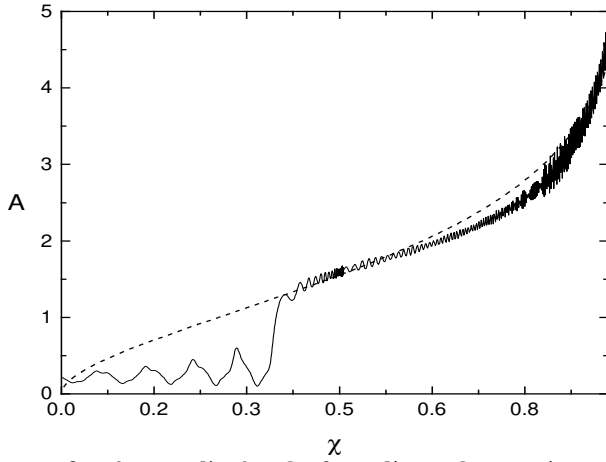


FIG. 3. The amplitude of a 2D soliton of attractive BEC as a function of the coefficient of nonlinearity, obtained by numerical solution of the GPE (1) (solid line), and as predicted by VA Eq.(8) (dashed line). VA adequately describes the dependence  $A(\chi)$  above the delocalizing transition point at  $\chi = 0.38$ .

An important remark concerning the Fig. 3 is that the VA fails to account for the delocalization of a soliton occurring when the norm drops below some critical value ( $\chi = 0.38$ , for  $\mu = 0.92$ ), which is manifested as a rapid spreading of the waveform.

## 2. Repulsive case

Similarly to the previous case, we generate a stable 2D soliton of repulsive BEC inserting the waveform Eq.(9) with  $A = 2.5$ ;  $a = 1.1$  as initial condition for the Eq.(3) with  $\mu = 4.0$  and  $\mu = 1$ . After some transition period a stable soliton is formed as shown in Fig.4. In this case the oscillations of the amplitude around the stable state is less pronounced due to repulsive nature of the condensate.

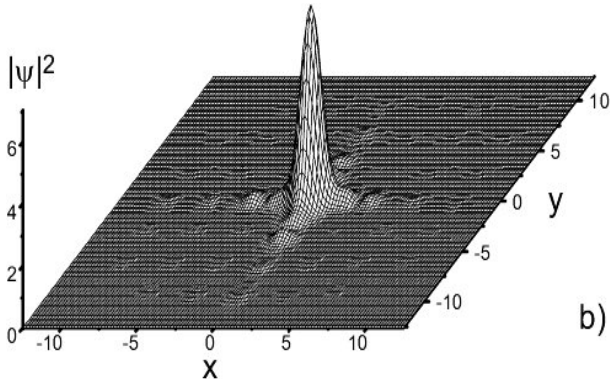
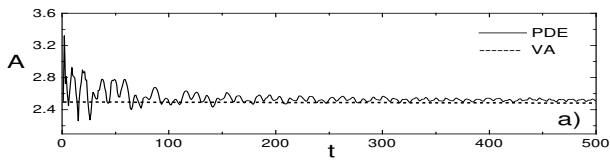


FIG. 4. Formation of a 2D soliton from the initial state given by Eq.(9) with  $A = 2.5$ ;  $a = 1.1$  in the OL of strength  $\mu = 4.0$ . a) Transient oscillations of the amplitude, b) stable 2D soliton of repulsive BEC. The norm has decreased by 50 % during the formation of a stable soliton.

The fact that the ansatz (9) properly accounts for the satellites can be seen from the comparison of contour plots in Fig.5.

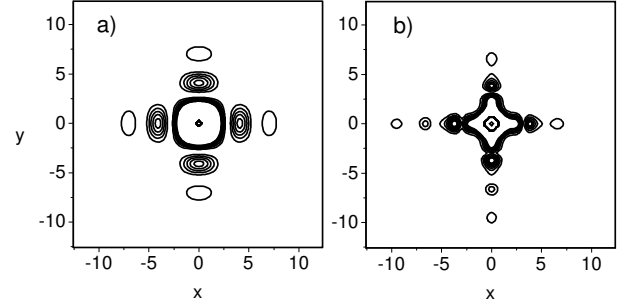


FIG. 5. Contour plots of the ansatz Eq.(9) (a), and the stable 2D soliton (b) of repulsive BEC.

Fig.6 illustrates the soliton's amplitude as a function of the strength of the OL given by VA Eq.(11), and obtained by direct numerical solution of Eq.(3).

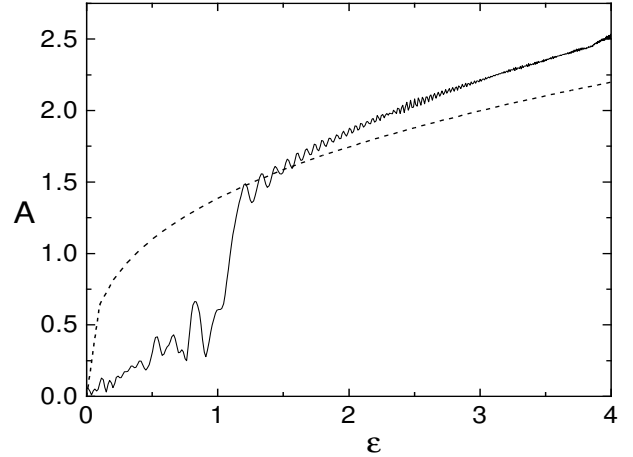


FIG. 6. The amplitude of a 2D soliton of repulsive BEC as a function of the strength of the periodic potential. Solid line - numerical solution of Eq.(3), dashed line - prediction of VA Eq.(11).

Here again, as in the attractive case, we see that the VA fails to predict the delocalizing transition (at  $\mu' = 1.2$ ). Below we consider in detail the delocalizing transition of multidimensional solitons in periodic potentials.

## III. DELOCALIZING TRANSITION

The delocalizing transition of solitons is manifested as irreversible transformation of the localized waveform to the extended state. The transition can be induced by

decreasing of the strength of the periodic potential, or reducing the coefficient of nonlinearity in Eq.(3), below some critical value. As pointed out in the previous section, the delocalizing transition of solitons is missed in VA description. In this section we present an interpretation of the phenomenon, involving the quantum bound states in the effective potential created by the soliton. For this we assume the condensate to have the form of a single cell soliton, and consider the VA equations valid until the delocalizing transition occurs. An example of this is shown in Fig. 3 for the case of attractive interactions. The underlying idea is to consider the GPE (3) as a linear Schrodinger equation with the effective potential

$$V_{\text{eff}} = V_{01} + j \bar{j}; \quad (12)$$

where  $V_{01}$  is the periodic potential of the OL, and the second term represents the contribution of the soliton. Finding the stationary solution of the Schrodinger equation with the potential (12) is similar to the self-consistent Hartree-Fock approximation of quantum mechanics. From this point of view it is clear that the existence of matter-wave solitons is linked to the existence of quantum bound states in the effective potential (12). We remark that the periodic part  $V_{01}$  can be eliminated from the effective potential. This is particularly connected to the possibility, that the GPE (1) with a periodic potential can be reduced to the standard NLSE in the effective mass formalism [19]. In other words, the contribution of  $V_{01}$  in the linear Schrodinger problem can be accounted in terms of an effective mass description for the extended states of the linear problem. These states have positive or negative effective masses depending on their interaction being, respectively, repulsive or attractive (they resemble electrons or holes of usual solids). In both cases we reveal that the effective potential reduces only to the soliton part with renormalized coefficient of nonlinearity [19]

$$V_{\text{eff}} = j \bar{j} (\mathbf{x}; \mathbf{y})^2; \quad (13)$$

where  $(\mathbf{x}; \mathbf{y})$  denotes the solution of the nonlinear problem in the presence of OL, evaluated at the delocalizing transition point. Notice that the effective potential is always negative, i.e. the soliton acts always as a potential well in the corresponding Schrodinger problem (in the repulsive case the sign of the potential is reversed by the negative effective mass). The problem then is to investigate the existence of states with negative energy of the following Schrodinger equation

$$(-\nabla^2 + V_{\text{eff}} - E) (\mathbf{x}; \mathbf{y}) = 0; \quad (14)$$

For this one can resort to numerical schemes for Eq. (14) to find that at the delocalization point the effective potential has the critical strength to support just a single bound state. In the following, however, we shall provide an analytical estimation of the number of bound states employing the VA solutions discussed in the previous sections and approximating the effective potential

with a solvable potential for which this number is exactly known. To this end we use the following Pöschl-Teller potential [20]

$$V_{\text{PT}}(r) = \frac{A^2}{\cosh(r - \frac{A^2}{2a \ln 2})^2}; \quad (15)$$

to approximate  $V_{\text{eff}}$  at the delocalization transition. The parametric form of  $V_{\text{PT}}$  is fixed so that  $V_{\text{PT}}$  has the same amplitude and the same integral value:  $2 \int_0^\infty r V_{\text{eff}}(r) dr$ , as for  $V_{\text{eff}}$ . In Fig. 7  $V_{\text{eff}}$  and its Pöschl-Teller approximation are depicted for the parameter values corresponding to the delocalization transition of Fig. 3.

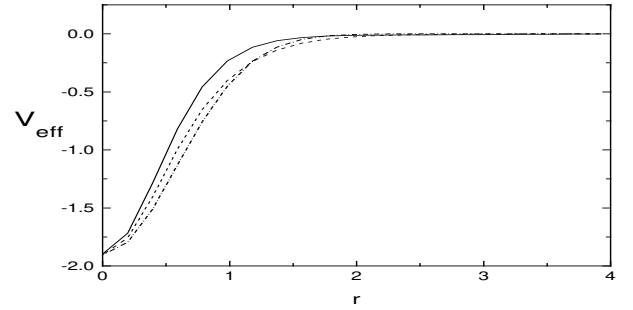


FIG. 7. The effective potential of a 2D soliton of attractive BEC at the delocalizing transition point, obtained from numerical solution of the GPE (3). The dashed line refers to the Pöschl-Teller potential in Eq. (15), while the dash-dotted line is the Gaussian approximation Eq.(7) with parameters  $A_d = 1.38$ ,  $a_d = 1.25$ , corresponding to the delocalizing transition point of Fig. 3 at  $\mu = 0.38$  for  $\beta = 0.92$ .

The number of bound states of the Pöschl-Teller potential is given by the integer part of  $n$  [21]

$$n = \frac{1}{4} \left( 1 + \frac{2 A^2}{a \ln 2} + 1 \right); \quad (16)$$

This equation can be reduced to a more convenient form by using the expressions for the amplitude  $A$  and the width  $a$  of the soliton as obtained from VA. At the delocalizing transition  $n = 1$  so that, after substitution  $A^2/a = N$ , the Eq.(16) reduces to  $\frac{N}{4} = \ln 2$ . This means that there exists a critical value  $N_{\text{cr}} = 4 \ln 2$  for the number of atoms, below which the soliton disintegrates (notice that this delocalization threshold is a factor of  $\ln 2$  smaller than that of unstable 2D Townes soliton [16]). Since  $N_{\text{cr}}$  is related to the amplitude and width  $A_d; a_d$ , of the soliton at the delocalization point by the variational equations, we can express the delocalization condition in terms of  $A_d; a_d$  as

$$N = \frac{1}{2} a_d^2 (1 - \ln 2) e^{1/a_d}; \quad \frac{A_d^2}{4 a_d} = \ln 2; \quad (17)$$

In the following we shall compare these expressions for the delocalization transition with the results of direct PDE simulations.

Since the 1D Schrodinger equation has bound state solution in any confining potential (even of infinitesimal depth), this implies that the delocalizing transition of bright solitons cannot occur in 1D case. It is interesting to start with consideration of this situation, since it provides more insight into the general problem.

The dynamics of the condensate is governed by 1D version of the GPE (3). The stationary localized solution to this equation can be found by standard numerical relaxation procedure. One of such gap soliton solutions for repulsive case ( $\gamma > 0$ ) is presented in Fig.8

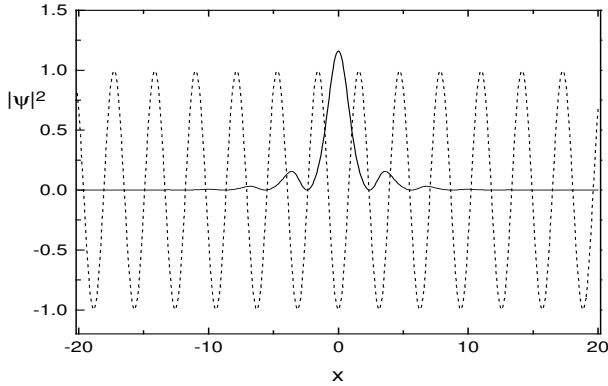


FIG. 8. The initial waveform corresponding to stationary solution of Eq.(3) with parameters  $\mu = 1$ ;  $\gamma = 1$ : Dashed line represents 1D OL potential  $V(x) = \cos(2x)$ :

Now we explore the behavior of 1D soliton under adiabatic variation of the strength of OL  $\mu(t)$  or coefficient of nonlinearity  $\gamma(t)$ , using the above solution (Fig.8) as initial condition for time-dependent GPE (3). We assume the simplest linear function for variation of the amplitude  $\mu(t) = \mu_0 f(t)$  and coefficient of nonlinearity  $\gamma(t) = \gamma_0 f(t)$ , with

$$f(t) = \begin{cases} 1 & \text{if } 0 \leq t \leq 0.5 t_{\text{end}} \\ 2 & \text{if } 0.5 t_{\text{end}} < t \leq t_{\text{end}} \end{cases} \quad (18)$$

In Fig.9 we report the transformation of the solitonic state into the extended one, and restoring its original shape as the strength of the OL is adiabatically decreased to zero at  $t = 50$ , and then increased back to initial value at  $t = 100$ .

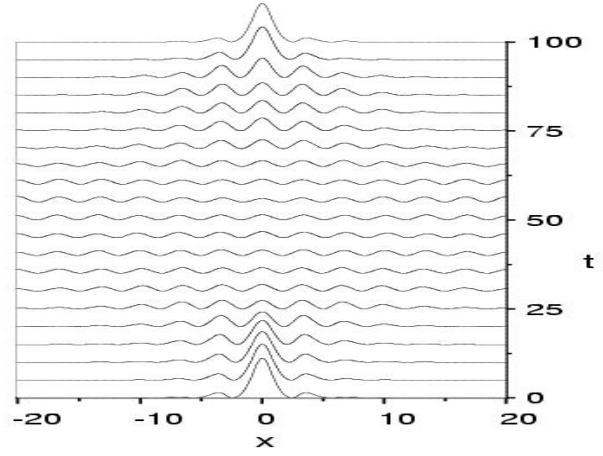


FIG. 9. When the strength of the OL  $\mu_0 = 1$  is decreased to zero at  $t = 50$  and then increased back to its initial value, the 1D gap soliton of repulsive BEC fully restores its original form.

The opposite situation also reveals the solitariness of the waveform (Fig.8). Specifically, when the strength of the OL is increased enough the BEC matter is entirely pulled into the central unit cell (Figs. 10, 11).

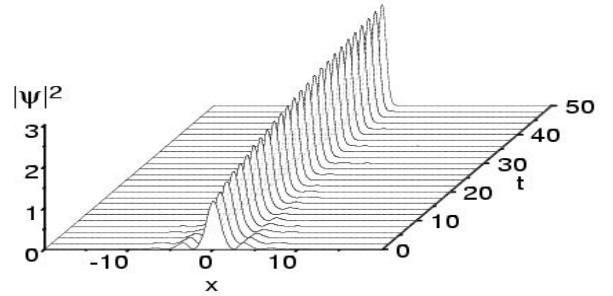


FIG. 10. All the BEC matter is pulled into the central unit cell as the strength of the OL is linearly increased from  $\mu = 1$  to  $\mu = 5$  during  $t = 50$ .

The following Fig.11 represents the waveform in OL potential at  $t = 50$ .

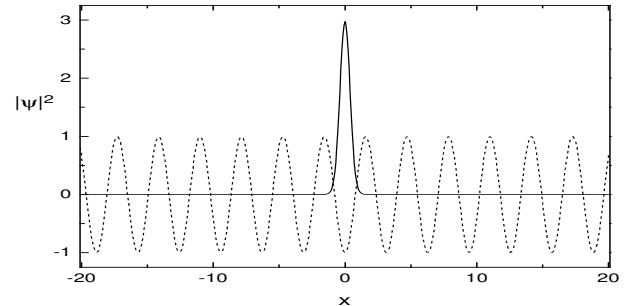


FIG. 11. A 1D gap soliton of Fig.8 contracts into the central unit cell when the strength of the OL is increased from  $\mu = 1$  to  $\mu = 5$ . Dashed line represents  $\cos(2x)$

In the case of attractive BEC ( $\gamma < 0$ ), the stationary solution of the GPE (3) can be found similarly to above,

by relaxation method. Below we consider the solution corresponding to the strength of the OL  $\mu = 1.0$ , and the soliton initially is a single cell of the periodic potential. Then we use this solution as initial condition for GPE (3) and observe the spreading and contracting of the waveform as the coefficient of nonlinearity is decreased to zero and increased back to its original value, as displayed in Fig.12

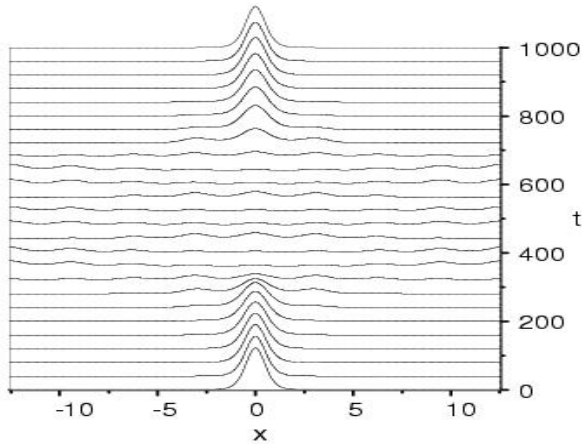


FIG. 12. Soliton of attractive BEC in 1D OL of strength  $\mu = 1$  retains its integrity while the coefficient of nonlinearity is decreased to zero at  $t = 500$ , and then increased back to the original value  $\mu = 1$  at  $t = 1000$ .

To conclude this subsection we note, that the bright solitons in 1D periodic potentials do not exhibit the delocalizing transition as the OL is weakened or the coefficient of nonlinearity is decreased. The integrity of solitons is manifested by recovering their original shape as the periodic potential or coefficient of nonlinearity is restored to the initial value. This is in agreement with the proposed physical mechanism associating the delocalizing transition with quantum bound states in the effective potential created by the soliton. As noted above, in 1D there are always bound states in the confining potential, and that is why the soliton doesn't disintegrate even when the depth of the effective potential becomes infinitesimal.

## B. 2D optical lattice

We separately consider the delocalizing transition of bright solitons of attractive and repulsive BECs in 2D OLs. Starting point in these cases, similarly to the previous situation, is construction of a stationary solitonic state in a 2D OL.

### 1. Attractive case

The stationary soliton of attractive BEC in 2D OL (Fig.2), generated from the Gaussian waveform with pa-

rameters prescribed by the VA was employed as initial condition in the GPE (3) with time-dependent parameters  $\mu(t)$ , or  $\chi(t)$ . By adiabatic variation of these parameters one can bring the soliton close to the delocalizing transition point, and then return back recovering the initial waveform, or induce the delocalizing transition by slightly more decreasing the critical parameter, as demonstrated in Fig.13 by numerical solution of the GPE (3).

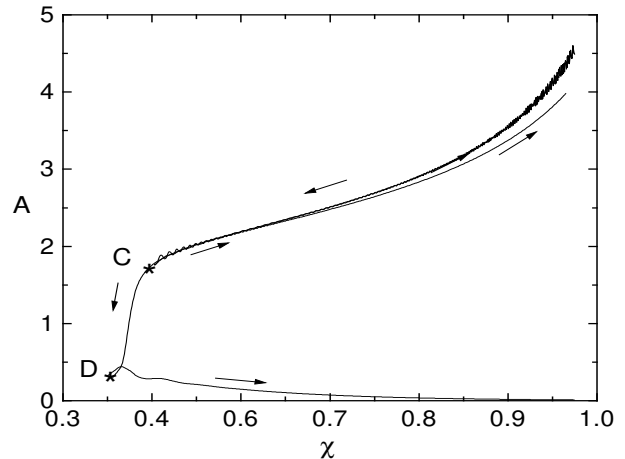


FIG. 13. A 2D soliton of attractive BEC recovers its original amplitude when the parameter  $\chi(t)$  is decreased and then increased back without crossing the critical value (near point C), and irreversibly disintegrates when crossed (point D). A small deficit in the return value of the amplitude is caused by the energy loss due to imperfect adiabaticity of the process.

Repeating similar delocalizing transition simulations one can establish the existence region of 2D solitons in the parameter space  $\mu$  vs.  $\chi$ . In Fig.14 we present the result of such numerical simulations for different strengths of the OL. Unlike the Fig.13, the coefficient of nonlinearity  $\mu(t)$  was linearly decreased until zero, as we are interested in the critical values  $\chi_c$  leading to delocalization of the soliton.

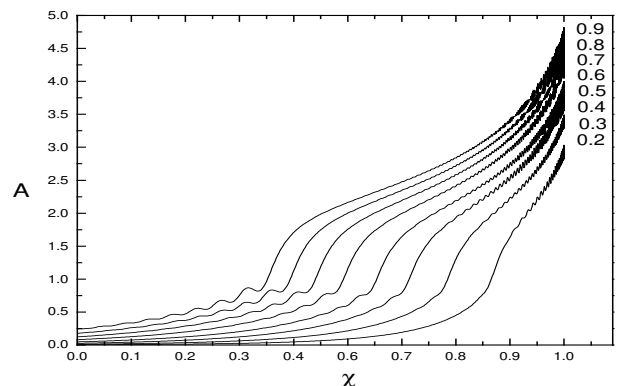


FIG. 14. Delocalizing transition of a 2D soliton in OLs of different strength  $\mu$  (shown to the right of corresponding curves).



Fig.15 represents the existence region for 2D solitons of attractive BEC in the OL.

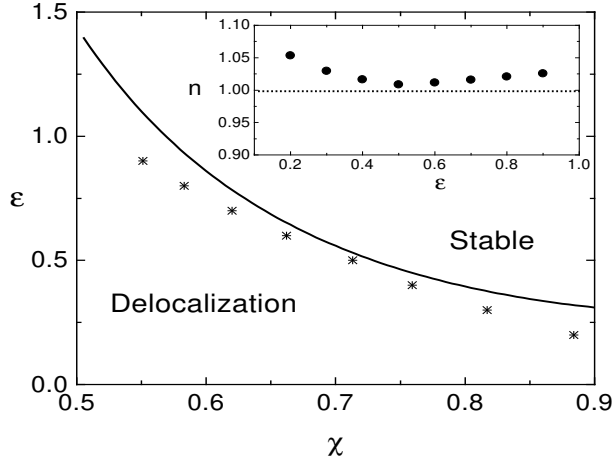


FIG. 15. The existence region of 2D solitons of attractive BEC. Solid line – parametric solution of Eq.(17), also using the conserved norm  $N = A_d^2 = a_d$ . Stars – delocalizing transition points of Fig.14. The inset shows the number of quantum bound states evaluated at the delocalizing transition points according to Eq.(16).

The number of quantum bound states in the effective potential at the point of delocalizing transition, evaluated from numerical simulations (Fig.14) and using the Eq.(16), appears to be very close to one (see the inset in Fig.15) for all values of  $\chi$ , which supports the proposed physical model.

## 2. Repulsive case

As pointed out, matter-wave solitons of repulsive BEC in OLs have a composite structure. The satellites are more pronounced when the soliton is driven close to the delocalizing transition point in the parametric space  $\chi$  vs.  $\epsilon$ , as illustrated in Fig.16.

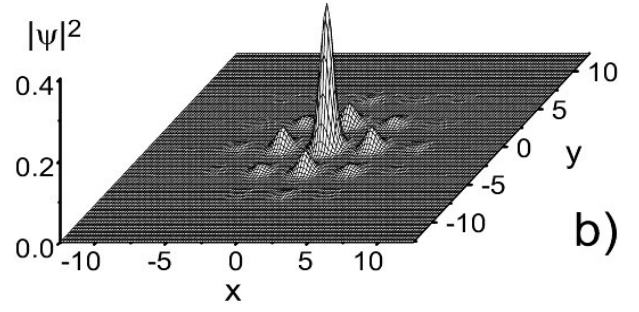
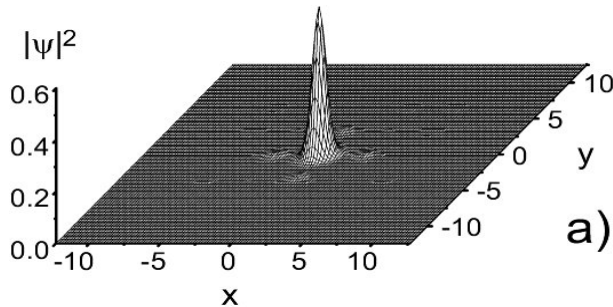


FIG. 16. a) A stable 2D soliton of repulsive BEC ( $\chi = 1$ ) in OL of strength  $\epsilon = 4.5$ . b) The satellites are more pronounced when the delocalizing transition point is approached by reducing the coefficient of nonlinearity until  $\epsilon = 0.4$ .

Similarly to attractive case, the soliton can be brought close to the delocalizing transition point by adiabatic change of parameters  $\epsilon$  or  $\chi$ . Then, if the initial values of parameters are restored without crossing the threshold, the soliton recovers its original shape, otherwise it irreversibly disintegrates. Such a numerical simulation with a soliton of repulsive BEC is presented in Fig.17.

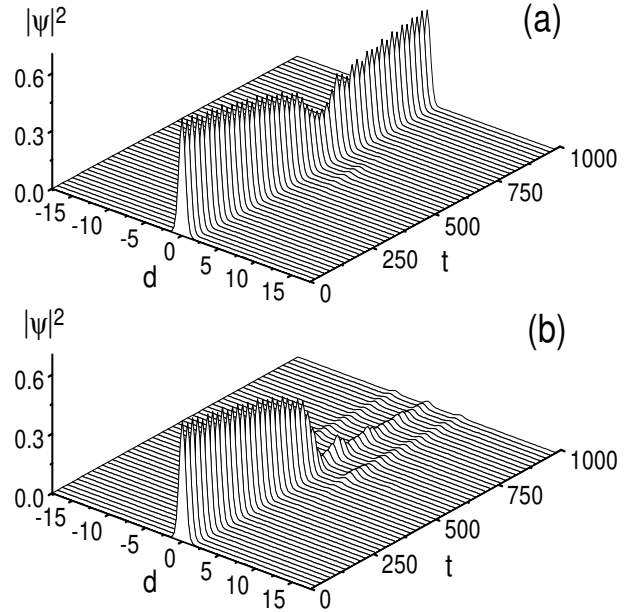


FIG. 17. Diagonal section profile for the time evolution of a 2D soliton according to GPE (3). (a) The waveform recovers its original shape when the magnitude of the periodic potential is linearly decreased from  $\epsilon_0 = 4.5$  until  $\epsilon_{min} = 3.42$  at  $t = 500$ , and then increased back to  $\epsilon_0$  at  $t = 1000$ . (b) Abrupt delocalizing transition occurs as the strength of the OL is lowered below the critical value  $\epsilon_c = 3.38$  at  $t = 500$ . The Eq.(18) for variation of  $\epsilon(t) = \epsilon_0 f(t)$  is applied with  $t_{end} = 1000$ , and  $\alpha = 0.25$  for (a),  $\alpha = 0.26$  for (b).

Of particular interest is the interplay between the central peak and satellites of the lattice soliton in repulsive BEC. Some information can be obtained by recording the

amount of BEC matter  $I(t)$  in the central peak (connected to a unit cell), while the parameters  $\mu$  or  $\lambda$  adiabatically varied in time.

$$I(t) = \sum_{j=-2}^2 \int_{-2}^2 |\psi(x,y;t)|^2 dx dy: \quad (19)$$

Time evolution of this quantity is presented in Fig.18

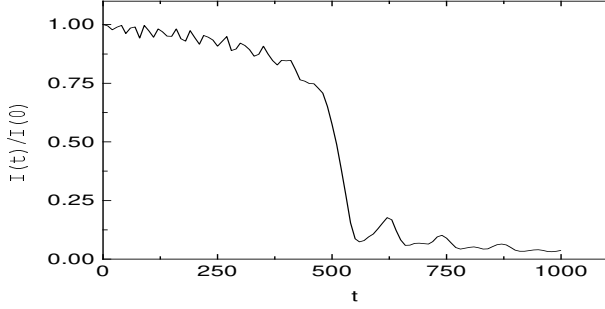


FIG. 18. Amount of BEC matter in the central peak of a 2D soliton according to Eq.(19), corresponding to Fig. 17b.

From this figure one can judge about the role of the central peak in the integrity of the soliton. The delocalizing transition of a composite soliton implies the rapid spreading of its central peak.

### C. 3D optical lattice

There is a growing interest in properties of BEC in 3D OLs [22,23]. The effect of dimensionality in the process of delocalizing transition of matter-wave solitons is of particular interest. Since we consider the phenomenon as rapid spreading of the wave-packet through tunneling of BEC into neighboring lattice sites, the main manifestation of the dimensionality should be the increased sharpness of the transition (because of more neighboring cells compared to 2D case).

To verify the above conjecture, we performed numerical simulation of the delocalizing transition of a soliton in 3D OL. The procedure for preparation of a stable soliton and subsequent adiabatic variation of system parameters are similar to 2D case. The result is presented in Fig.19. As expected, the delocalizing transition in 3D appears to be more sharp compared to 2D case.

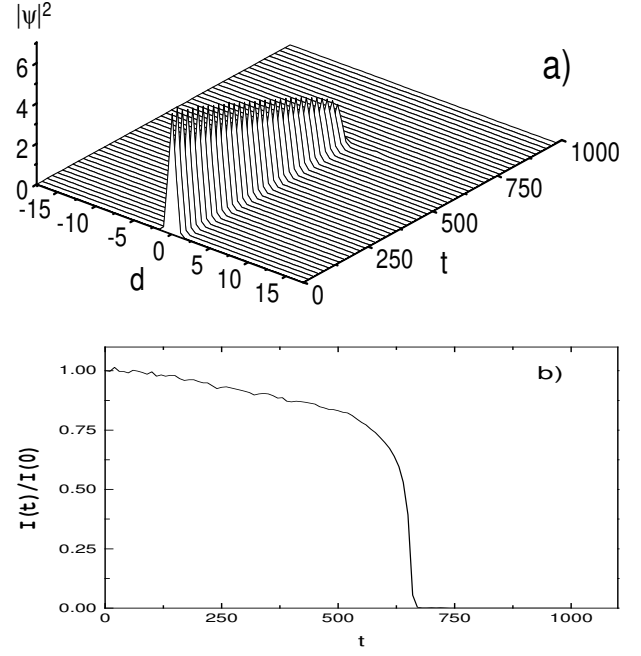


FIG. 19. Wave profile along the main diagonal of a cubic domain  $x,y,z \in [-4,4]$  as obtained by numerical solution of the GPE (3) with  $\mu(t) = \mu_0 (1 - t/t_{end})$  (a), and corresponding integral Eq.(19) over the central unit cell (b), for a 3D OL with  $\mu_0 = 4.5$ ;  $\lambda = 1.0$ ;  $t_{end} = 1000$ .

Also note the absence of transient oscillations of the integral atomic number after delocalizing transition in Fig.19b, as opposed to 2D case (Fig.18). This is another effect of higher dimensionality.

## IV. EXPERIMENTAL FEASIBILITY

Addressing the possibility of experimental observation of phenomena considered in this paper, we note the rapid progress in manipulation techniques for BEC in OLs [22-24]. However, the matter-wave solitons in periodic potentials of OLs have not been experimentally realized yet. Different approaches were proposed, of which particular interest is the generation of gap solitons in repulsive BEC employing the phenomenon of modulational instability [5,6]. Another possibility is the independent successive formation of BEC in single sites of the OL as proposed in Ref. [26]. The BEC initially occupying a single or few lattice sites of the periodic potential quickly transforms into the solitonic waveform (certainly, if the parameters are in the existence region), as revealed from the numerical simulations.

After the matter-wave soliton is created, the delocalizing transition can be induced by decreasing the strength of the OL through the intensity of laser wave, or reducing the coefficient of nonlinearity by changing the atomic scattering length via the Feshbach resonance. The signature of the phenomenon is sudden disintegration of

the soliton at the critical point, therefore it will be accompanied by dropping of the atomic density, which can be detected by imaging techniques. The resolution of absorption-imaging systems currently in use (which is  $7 \text{ nm}$  [25]) is sufficient for controlling the properties of BEC in the range of a unit cell of the OL.

Now let us estimate the dimensionless parameters in physical units. In typical experiments to date the relevant parameters are given by  $n_0 = 10^{20} \text{ m}^{-3}$ ,  $a_s = 5.4 \text{ nm}$ , and  $k_L = 2 \pi / \lambda = 8.06 \cdot 10^6 \text{ m}^{-1}$  for Rb [27], and  $n_0 = 3 \cdot 10^{21} \text{ m}^{-3}$ ,  $a_s = 2.65 \text{ nm}$ , and  $k_L = 1.07 \cdot 10^7 \text{ m}^{-1}$  for Na [28]. The strength of nonlinear atomic interaction is given by  $\mu = 8 \pi n_0 a_s \hbar^2 k_L^2 = 0.21$  for Rb, and  $\mu = 1.76$  for Na. Higher or lower values of  $\mu$  may be achieved by changing the density of the condensate  $n_0$ , atomic scattering length  $a_s$ , or  $k_L$ . All three parameters can be changed independently. The strengths of OLs considered above are in the range of usual experimental conditions [29]  $\mu = 0 \dots 20$  in units of recoil energy  $E_{\text{rec}} = \hbar^2 k_L^2 / (2m)$ . Our numerical simulation time step  $\sim 1000$ , well satisfying the adiabaticity condition, correspond to  $\sim 0.5 \text{ s}$ . The average lifetime of BEC in optical trap, limited by three-body collisions and off-resonant scattering of lattice photons is more than  $3 \text{ s}$  [30]. Therefore, observation of the delocalizing transition of solitons is possible in the present experimental conditions.

## V. CONCLUSIONS

We have studied the existence and delocalizing transition of multidimensional solitons in periodic potentials by means of the VA and direct numerical integration of the Gross-Pitaevskii equation. VA provides the initial configuration for the soliton parameters which can be used in PDE to generate a stable multidimensional soliton.

The most interesting property of multidimensional (2D and 3D) solitons observed in this study is the delocalizing transition, which is manifested as irreversible disintegration of the soliton at some critical strength of the periodic potential, or coefficient of nonlinearity. Contrarily, 1D solitons do not exhibit the delocalizing transition, retaining their integrity over the whole range of parameter variations.

We proposed a physical mechanism for delocalizing transition of solitons, according to which the existence of a soliton is associated with the existence of quantum bound states in the effective potential created by the soliton. At the point of delocalizing transition, the effective potential has the critical strength to support only a single bound state. As the strength becomes weaker than the critical value, the effective potential cannot support a bound state, and as a consequence, the soliton irreversibly disintegrates. Using the exactly solvable Pöschl-Teller potential as approximation for the effective potential created by the soliton, we analytically determined the existence region for 2D solitons. Numerical simula-

tions of the Gross-Pitaevskii equation have confirmed the validity of the proposed model.

Although we considered the problem with the emphasis on Bose-Einstein condensates in OLs, multidimensional solitons and the phenomenon of delocalizing transition can be observed in other relevant systems, e.g. optically induced nonlinear waveguide arrays [31].

## ACKNOWLEDGEMENTS

We acknowledge interesting discussions with J.C. Eilbeck, S. De Filippo, and B.A. Malomed. B.B. thanks the Physics Department of the University of Salerno, Italy, for a two years research grant during which this work was done. M.S. acknowledges partial support from a MURST-PRIN-2000 Initiative, and from the European grant LOCNET no. HPRN-CT-1999-00163.

---

<sup>y</sup> Permanent address: Physical-Technical Institute, 2-b, Mavllyanov str., 700084, Tashkent, Uzbekistan.

- [1] L. Khaykovich et al., Science 296, 1290, (2002); K.E. Strecker et al., Nature 417, 150, (2002).
- [2] S. Burger et al., Phys. Rev. Lett. 83, 5198 (1999); J. Denschlag et al., Science, 287, 97 (2000).
- [3] L.D. Carr, Y. Castin, Phys. Rev. A 66, 063602 (2002); U.A. Khawaja et al., Phys. Rev. Lett. 89, 200404 (2002); V.Y.F. Leung et al., Phys. Rev. A 66, 061602 (2002); L. Salasnich, A. Parola, and L. Reatto, Phys. Rev. A 66, 043603 (2002).
- [4] O. Zobay et al., Phys. Rev. A 59, 643 (1999); S. Potting et al., J. Mod. Opt. 47, 2653 (2000).
- [5] V.V. Konotop and M. Salerno, Phys. Rev. A 65, 021602 (2002); G.L. Al'mov, V.V. Konotop, and M. Salerno, Europhys. Lett. 58, 7 (2002); K.M. Hilligs, M.K. Oberthaler, and K. Marzlin, Phys. Rev. A 66, 063605 (2002); G.L. Al'mov et al., Phys. Rev. E 66, 046608 (2002); P.J.Y. Louis et al., Phys. Rev. A 67, 013602 (2003).
- [6] B.B. Baizakov, V.V. Konotop, and M. Salerno, J. Phys. B 35, 5105 (2002).
- [7] E.A. Ostrovskaya and Y.S. Kivshar, e-print cond-mat/0303190.
- [8] B.B. Baizakov, B.A. Malomed, and M. Salerno, Europhys. Lett. 2003 (submitted).
- [9] G.K. Aloskas, K.O. Rasmussen, and A.R. Bishop, Phys. Rev. Lett. 89, 030402 (2002).
- [10] D. Jaksch et al., Phys. Rev. Lett. 81, 3108 (1998).
- [11] B.A. Malomed et al., JOSA B 16, 1197 (1999).
- [12] F. Dalfovo, S. Giorgini, L.P. Pitaevskii, and S. Stringari, Rev. Mod. Phys. 71, 463 (1999).
- [13] D. Anderson, Phys. Rev. A 27, 1393, 1983.
- [14] B.A. Malomed, Progr. Optics 43, 69 (2002).
- [15] F.Kh. Abdullaev, et al. Phys. Rev. A 67, 013605 (2003).

- [16] L. Berge, *Phys. Rep.* 303, 260 (1998).
- [17] M. G. Vakhitov and A. A. K obkolov, *Radiophys. Quantum Electron.* 16, 783 (1973).
- [18] W. H. Press, S. A. Teukolsky, W. T. Vetterling, and B. P. Flannery, *Numerical Recipes. The Art of Scientific Computing.* (Cambridge University Press, 1996).
- [19] M. J. Steel and W. Zhang, eprint cond-mat/9810284; H. Pu, et al. *Phys. Rev. A* 67, 043605 (2003).
- [20] G. Poschl and E. Teller, *Z. Phys.* 83, 1439 (1933).
- [21] S. Flugge *Practical Quantum Mechanics*, Springer-Verlag, 1994.
- [22] M. G reiner et al. *Nature*, 415, 39 (2002).
- [23] M. G reiner et al. *Nature*, 419, 51 (2002).
- [24] J. H. D enschlag et al. *J. Phys. B* 35, 3095, (2002).
- [25] S. Burger et al. *Phys. Rev. Lett.* 86, 4447 (2001).
- [26] S. Burger et al. *Europhys. Lett.* 57, 1 (2002).
- [27] E. A. Burt et al. *Phys. Rev. Lett.* 79, 337 (1997).
- [28] S. Inouye et al. *Nature*, 392, 151 (1998).
- [29] O. M orsch et al. *Phys. Rev. A* 67, 031603 (2003).
- [30] M. D. Barrett, J. A. Sauer, and M. S. Chapman, *Phys. Rev. Lett.* 87, 010404 (2001).
- [31] J. Fleisher et al. *Nature*, 422, 147 (2003); J. Fleisher et al. *Phys. Rev. Lett.* 90, 023902 (2003);